Available online at www.sciencedirect.com
ScienceDirect
Nanomedicine: Nanotechnology, Biology, and Medicine 4 (2008) 49–56
nanomedicine
www.nanomedjournal.com

Original Article: Experimental

Fluorescence intensity and lifetime imaging of free and micellar-encapsulated doxorubicin in living cells

Xiaowen Dai, BEng,[a] Zhilian Yue, PhD,[a] Mark E. Eccleston, PhD,[b] Johannes Swartling, PhD,[a] Nigel K.H. Slater, PhD,[a] Clemens F. Kaminski, PhD[a,*]

[a]*Department of Chemical Engineering, University of Cambridge, Cambridge*
[b]*Vivamer Ltd., Cambridge, United Kingdom*

Abstract Frequency domain fluorescence lifetime imaging microscopy (FLIM) has been used in combination with laser scanning confocal microscopy to study the cellular uptake behavior of the antitumor drug doxorubicin (DOX) and micellar-encapsulated DOX (PLyAd-DOX). The endocytosis uptake process of PLyAd-DOX was monitored over 72 hours using confocal microscopy, with a maximum fluorescence recorded at incubation periods around 24 hours. The micellar structure was not found to release the encapsulated DOX during the time course of imaging. FLIM revealed single lifetime distributions of PLyAd-DOX during accumulation in the cytoplasm. The free DOX in contrast was observed both in the cytoplasm and the nuclear domain of the cell, showing bimodal lifetime distributions. There was a marked dependence of the measured free-DOX lifetime on concentration within the cell, in contrast to reference experiments in aqueous solution, where no such dependence was found. The results suggest the formation of macromolecular structures inside the living cells.

Key words: Confocal microscopy; Fluorescence lifetime imaging; Doxorubicin; Polymeric micelles

Polymer systems are increasingly being recognized for their potential as delivery devices for existing drugs to improve their therapeutic efficacy. Drugs can be loaded by chemical conjugation or physical encapsulation, and the resulting nanoscale macromolecular prodrugs have demonstrated a number of advantages over small-molecular-weight drugs, notably prolonged plasma half-lives, selective accumulation in tumors, and sustained drug release over extended periods.[1-8] Functionality of these prodrugs can be finely tuned because of the inherent versatility in polymer chemistry. Much effort has been focused on the development of novel amphiphilic polymers, exhibiting a finely tuned balance of hydrophilicity and hydrophobicity. Such systems tend to self-assemble into nanostructures with hydrophobic cores and hydrophilic shells, systems that are particularly promising for the delivery of hydrophobic antitumor agents in cancer chemotherapy.[9-11]

A challenge in the design of macromolecular prodrugs is to ensure an efficient intracellular release of the carried drugs, which is a key requirement for their therapeutic efficacy. Unlike small molecular drugs, macromolecular prodrugs generally enter cells via endocytosis, and they are compartmentalized in the endosome and lysosome. An understanding of their intracellular fate after uptake is important in providing guidance for the design of efficient drug delivery systems. Key to this is the ability to differentiate between conjugated or encapsulated forms of drug and the free released drug inside living cells. Many anticancer drugs are intrinsically fluorescent, such as doxorubicin (DOX), which makes them convenient for probing and visualization with various microscopic

Received 7 July 2007; accepted 11 December 2007.
Xiaowen Dai is sponsored by the Cambridge Overseas Trust and the Engineering and Physical Sciences Research Council (EPSRC).
Clemens Kaminski gratefully acknowledges personal sponsorship from the Leverhulme Trust. The authors acknowledge the support of Vivamer Ltd. for providing us with doxorubicin samples used in this work.
*Corresponding author: Department of Chemical Engineering, University of Cambridge, Cambridge, United Kingdom.
E-mail address: cfk23@cam.ac.uk (C.F. Kaminski).

1549-9634/$ – see front matter © 2008 Elsevier Inc. All rights reserved.
doi:10.1016/j.nano.2007.12.002

Please cite this article as: X. Dai, Z. Yue, M.E. Eccleston, J. Swartling, N.K.H. Slater, C.F. Kaminski, Fluorescence intensity and lifetime imaging of free and micellar-encapsulated doxorubicin in living cells, *Nanomedicine: NBM* 2008;4:49-56, doi:10.1016/j.nano.2007.12.002

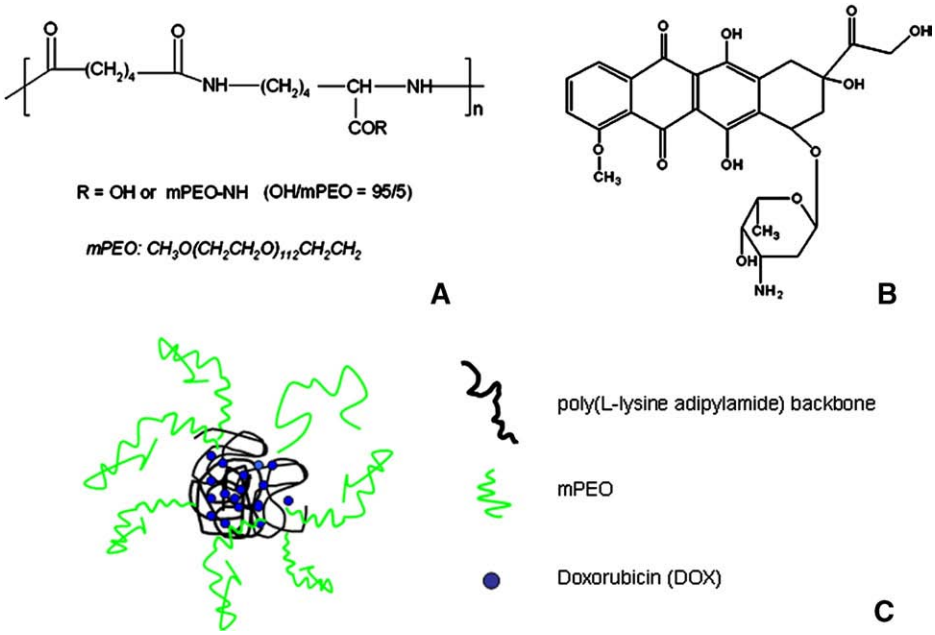

Figure 1. Chemical structures of PEGylated poly(L-lysine adipamide) (PLyAd) (**A**), doxorubicin (DOX) (**B**), and schematic representation of PLyAd-DOX-encapsulated structure (**C**).

imaging technologies. However, conventional intensity-based microscopic techniques are of limited value in this respect, because the intensity or spectral response does not differ significantly between polymeric and free-drug systems, thus making their differentiation inside the cells difficult. In this article we demonstrate the potential of fluorescence lifetime imaging microscopy (FLIM) as a tool for successfully distinguishing between polymer-mediated and free drug inside living cells. The fluorescence lifetime is sensitively dependent on the local physicochemical environment of a fluorophore. It probes the average time a molecule stays in its excited state before returning to the ground state, yielding information on intramolecular interactions, such as protein binding events,[12,13] changes in pH,[14] local viscosities,[15] the presence of quenchers such as oxygen or ions,[16,17] and many other parameters. FLIM is thus able to provide information on drug delivery candidates that other techniques cannot. To the best of our knowledge, the use of FLIM has not been reported in the literature in the specific context of drug delivery research. Partly this is because traditional implementations of FLIM, such as time-correlated single-photon counting (TCSPC) and time-gated detection, require the use of expensive laser and detector equipment. Equally importantly, these techniques require high photon fluxes, with associated increases in signal acquisition times, thus reducing their ability to track dynamic changes.

In this article we demonstrate what we believe to be the first application of FLIM in polymer-mediated drug delivery research. In particular we have set up a frequency domain widefield FLIM system, which makes use of inexpensive light-emitting diodes (LEDs) as excitation sources. The system is photon-efficient, and because lifetime information is tracked for all image pixels in parallel, measurements have good temporal resolution, making the technique suitable for dynamic studies in live cell systems. The system operates using an LED, the amplitude of which is modulated at a frequency of 40 MHz. Lifetimes are obtained using a homodyne detection scheme and extracting phase shift and demodulation information of the emitted fluorescent intensity from each individual image pixel. The technique is simple to implement and makes use of LEDs with high brightness, and a large emission area. Their spectral and illumination properties make them ideally suited for widefield FLIM to provide reliable lifetime information at sub-second data acquisition speed, which makes the technique ideally suited for dynamic imaging over extended observation periods.

The drug carrier studied in the present work was a grafted pseudopeptide, poly (L-lysine adipamide) with poly(ethylene glycol) side chains (PLyAd) (Figure 1). This amphiphilic synthetic polymer self-assembles into a core-shell-like structure with DOX encapsulated in its core. Here we present the first example of using LED-based frequency domain FLIM in the study of the intracellular dynamics of free DOX and of polymeric micellar-encapsulated DOX (PLyAd-DOX).

Methods

Materials

Doxorubicin hydrochloride (DOX.HCl) was obtained from Fluka (Gilingham, United Kingdom). Poly(L-lysine adipamide), prepared from an interfacial polymerization,[18] was treated in dimethyl sulfoxide (DMSO) with methoxypoly (oxyethylene) amine (Molar mass M_n = 4400 g mol^{-1}, 0.05

molar equivalent of [COOH]), in the presence of *N*,*N*′-dicyclohexylcarbodiimide and 4-dimethylaminopyridine. The product was purified by diafiltration (MWCO 5,000 Da, Millipore, Watford, United Kingdom) against four volumes of deionized water, before lyophilization to fine white powder. The structure of PLyAd was confirmed by ^{1}H nuclear magnetic resonance in d_6-DMSO.

In the presence of triethyl amine (100 μL), 25 mg of PLyAd and 5 mg of DOX.HCl were dissolved in DMSO (12.5 mL). An equal volume of deionized water was added and the mixture stirred at room temperature (18-23°C) for 1 hour, dialyzed (MWCO 12,000 Da) against deionized water for 72 hours to remove the DMSO, triethyl amine, and free DOX, before lyophilization to a red powder occurred.

Determination of drug loading

After dissolving 1 mg of PLyAd-DOX in 1 mL of DMSO, its absorption at 485 nm was measured on a Shimadzu UV-160A spectrophotometer (Milton Keynes, United Kingdom). The amount of DOX in PLyAd-DOX was quantified to be 5.1 wt%, based on a standard curve of DOX.HCl.

Steady-state fluorescence spectroscopy

The fluorescence spectra of free DOX and PLyAd-DOX in aqueous solutions were collected using a SPEX FluoroMax-3 spectrofluorometer (Horiba Jobin Yvon, Middlesex, United Kingdom).

Cell culture and sample preparation

Human cervical carcinoma (Hela) cells were grown in Dulbecco's modified Eagle's medium (DMEM; GIBCO, Paisley, United Kingdom) supplemented with 10% fetal bovine serum (GIBCO). Cells were maintained in a humid incubator at 37°C and with 5% CO_2 For living-cell fluorescence microscopy, cells were seeded into sterilized glass-bottom dishes (Mat-Tek, Ashland, Massachusetts) a day in advance.

Time-correlated single-photon counting

TCSPC lifetime measurements were performed at the Department of Physics, Politecnico di Milano, Italy. Free DOX at a concentration of 0.01 mg mL^{-1} in aqueous solution in standard 10-mm quartz cuvettes was measured. Picosecond light pulses at 535–545 nm were selected using an optical bandpass filter from a supercontinuum pulse-train generated by a self-mode-locked Ti-sapphire laser and a photonic crystal fiber.[19] The fluorescence decay curve was measured with a spectrally resolved TCSPC setup consisting of a spectrometer, a 32-channel photomultiplier tube (H7260-L32; Hamamatsu, Milan, Italy), a router (PML; Becker & Hickl Berlin, Germany), and a personal computer card with the TCSPC electronics (SPC-600; Becker & Hickl). The temporal resolution of the setup was 0.16 nanoseconds. The lifetime was determined by fitting an exponential, convolved with the instrument response function, to the measured decay curve.

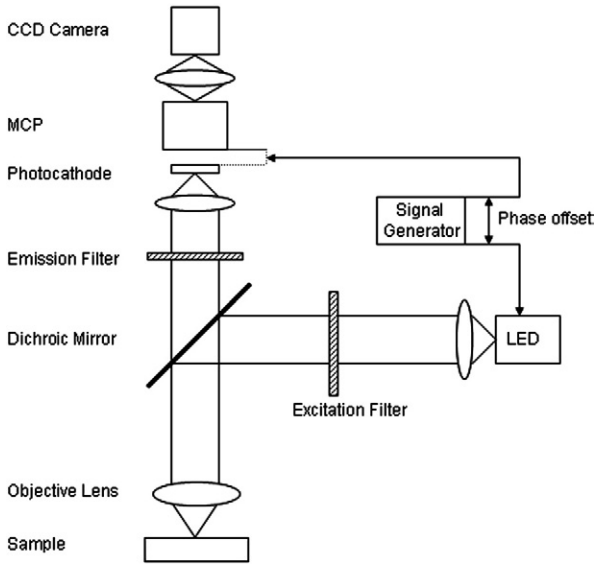

Figure 2. Diagram illustrating the main components of the frequency domain FLIM setup. The voltage on the photocathode of the multichannel plate intensifier is modulated at a frequency of 40 MHz. The same waveform was used to modulate the intensity of the light-emitting diode, but a variable phase shift could be imposed with respect to the excitation waveform, using a precision delay generator. For all the experiments reported here, 12 images were recorded for each cycle corresponding to 30-degree shifts between individual measurements. τ_ϕ and τ_m could thus be evaluated from sinusoidal fits through the 12 intensity values obtained for each pixel.

Laser scanning confocal microscopy

Laser scanning confocal microscopy (Olympus FV300, Olympus, Southall, United Kingdom) was used to study the dynamics of PLyAd-DOX uptake by the Hela cells using a conventional intensity-based approach. For this purpose cells were kept on a heater stage at 37°C and imaged with a 60× oil immersion objective (1.35 numerical aperture; Olympus). The 488-nm line from an argon ion laser was used for excitation, and emission was collected between 565 and 630 nm.

DOX and PLyAd-DOX were dissolved in phenol red–free DMEM (GIBCO) containing 30 mM HEPES buffer (GIBCO), 2.0 mM L-glutamine (GIBCO) and 10% fetal syringe filters for sterilization before experiments were started. Hela cells were incubated with 0.1 mg mL^{-1} PLyAd-DOX and imaged by confocal microscopy every 12 hours over periods lasting up to 72 hours.

Fluorescence lifetime imaging microscopy

Figure 2 shows the setup used for the FLIM measurements. The system was set up on an Olympus IX50 inverted microscope (Olympus, UK). As an excitation source, a 480-nm LED emitting over 40-nm bandwidth (Luxeon III star; Lumileds Lighting, San Jose, California) was fitted into the lamp housing in place of the standard mercury burner, with the LED light passing through the normal collector and condenser optics present in the microscope. Excitation and

emission wavelengths were selected using a 470- to 490-nm bandpass excitation filter, a 505-nm dichroic mirror, and a 545- to 580-nm bandpass emission filter. Fluorescence emission was detected using a Generation 2 type multichannel plate intensifier unit (II18MD; Lambert Instruments, Leutingewolde, The Netherlands), which was optically coupled to a charge-coupled device camera (CCD-1300D; VDS Vosskuhler, Osnabruck, Germany). The LED intensity and the detector intensifier gain were both modulated at a frequency of 40 MHz using a signal generator/phase shifter (LIFA modulation signal generator; Lambert Instruments).

In frequency-domain FLIM, excitation with a time-modulated intensity leads to a phase shift (ϕ) of the fluorescence waveform and a demodulation (m) of the emitted light with respect to the excitation waveform. For each pixel, 12 images were recorded at different phase positions over a full modulation cycle, in a scheme analogous to homodyne detection. To obtain a standard against which lifetime measurements could be calibrated, a 1.0 μM solution of rhodamine 6G was prepared in water, providing a reference lifetime standard of 4.11 nanoseconds. The calibration protocol and a full discussion on the precision and accuracy of the technique are described elsewhere.[17,20] Using a lifetime standard as a reference permits us to account for hardware-induced phase shifts and demodulations introduced by the electronics and optics inserted in the signal path in a convenient manner. The fluorescence lifetimes were calculated by fitting a sine wave function through the sequence of recorded intensities in each pixel using the following equations:

$$\tau_\phi = \frac{1}{\omega}\tan\left[\left(\phi - \phi_{ref}\right) + \tan^{-1}\left(\omega\tau_{ref}\right)\right] \quad (1)$$

$$\tau_m = \frac{1}{\omega}\left[\frac{m_{ref}^2}{m^2}\left(1+\omega^2\tau_{ref}^2\right) - 1\right]^{1/2} \quad (2)$$

where τ_ϕ and τ_m refer to the phase and modulation lifetimes, respectively, and ϕ_{ref}, m_{ref} and τ_{ref} refer to the phase shift, demodulation, and lifetime of the reference sample. Eq 1 and 2 are parametrically independent, and thus lifetimes can be independently calculated for τ_ϕ and τ_m, but only in the case of single exponential fluorescence decays is τ_ϕ found to be equal to τ_m.[21]

For the lifetime measurements, cells were incubated with 0.01 and 0.05 mg mL^{-1} free DOX and PLyAd-DOX for 24 hours before imaging. The concentration of PLyAd-DOX (1.0 mg mL^{-1}) was adjusted to yield a DOX concentration of 0.05 mg mL^{-1}. Lifetime images were recorded using a 100× oil immersion objective (1.4 numerical aperture; Olympus).

Results

Figure 3 shows the absorption spectrum of free DOX as well as the emission spectra of both free DOX and PLyAd-DOX on excitation near 485 nm. For both systems the emitted fluorescence peaks near 595 nm. The fluorescence lifetime of free DOX in aqueous solution was measured using TCSPC. We obtained a concentration-independent single exponential decay corresponding to a lifetime of 1.1 nanoseconds for free DOX.

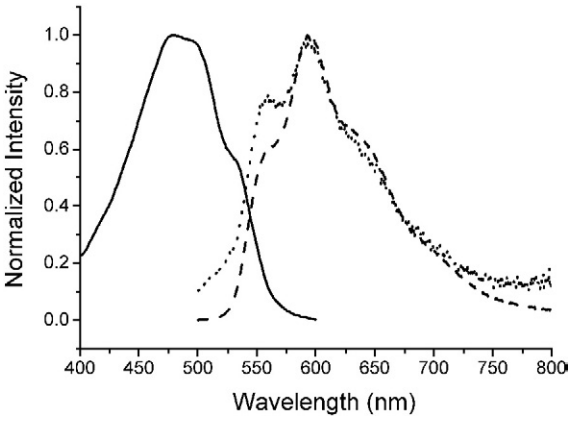

Figure 3. Absorption (––) and emission (–––––) spectra of 0.01 mg mL^{-1} free DOX, and emission spectrum of 0.2 mg mL^{-1} PLyAd-DOX (····), all in aqueous solution.

Cells were incubated with 0.1 mg mL^{-1} PLyAd-DOX in a glass-bottom dish and imaged using 488-nm excitation light. The fluorescence emission from PLyAd-DOX was collected between 565 and 630 nm using the laser scanning confocal microscope after incubation periods of 4, 12, 24, 48, and 72 hours (Figure 4), respectively. Fluorescence yields were obtained by normalizing integrated fluorescence intensities to the cellular area (indicated by transmission microscopy). The data were used to quantify the cellular uptake of PLyAd-DOX as a function of time. It is evident from the images shown in Figure 4 how PLyAd-DOX gradually accumulated in the cytoplasm without evidence of entering into the nucleus, from which no signals were obtained. The fluorescence yield seemed to increase with time, reaching a maximum after about 24 hours of incubation, followed by a gradual decrease (Figure 4, *K*).

Fluorescence lifetime images were obtained from DOX in live Hela cells. The results are shown in Figure 5, depicting intensity images in the first column, lifetime images in the second column, and lifetime histograms in the third column. Image series *A–C* and *D–F* show data of free DOX, and series *G–I* show the data of PLyAd-DOX. It can be seen that the free DOX is translocated into the nucleus, whereas PLyAd-DOX is not.

Free DOX displayed very strong nuclear accumulation after 24 hours of incubation (Figure 5, *A*, *D*). It is clearly seen in the lifetime images (Figure 5, *B*, *E*) that there exist lifetime differences between the nuclear domains and the cytoplasm. These bimodal distributions are clearly exhibited also on the lifetime histograms (Figure 5, *C*, *F*), which show significant shifts toward longer lifetimes in the nucleus as compared with the cytoplasm. For example,

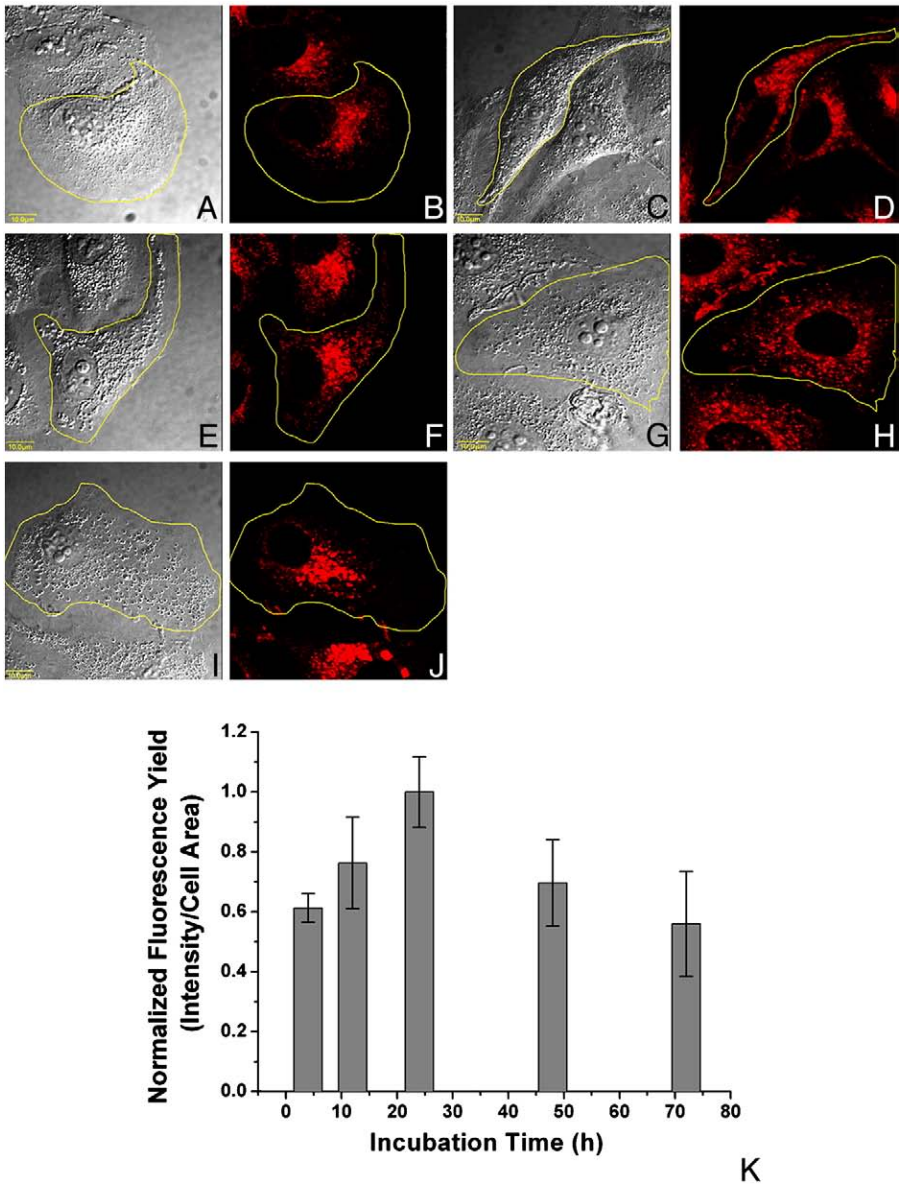

Figure 4. Uptake of PLyAd-DOX by Hela cells as imaged with confocal microscopy. Cells were incubated with 0.1 mg mL^{-1} PLyAd-DOX for 4 hours (**A, B**), 12 hours (**C, D**), 24 hours (**E, F**), 48 hours (**G, H**), and 72 hours (**I, J**). **A**, **C**, **E**, **G**, and **I** are bright-field images of the cells, and **B**, **D**, **F**, **H**, and **J** are fluorescent images of the same field. The yellow line is used to demarcate an outline of the cells. **K**, Time history of PLyAd-DOX fluorescence yield, which peaks near 24 hours.

cells incubated with 0.01 mg mL^{-1} DOX displayed lifetimes of 1.8 nanoseconds in the cytoplasm compared with 3.5 nanoseconds in the nucleus (Figure 5, *B*, *C*). At higher incubation concentrations (0.05 mg mL^{-1}) the lifetimes were measured to be 1.8 nanoseconds in the cytoplasm and 2.8 nanoseconds in the nucleus, respectively (Figure 5, *E*, *F*).

The concentration of PLyAd-DOX was adjusted to yield a DOX concentration of 0.05 mg mL^{-1}. The PLyAd micellar prodrug reduced the cytotoxicity of the drugs, and cellular viability was found to be much higher than the cells incubated with 0.05 mg mL^{-1} free DOX. It appears from Figure 5, *G* that PLyAd-DOX is taken up by endocytosis and subsequently localized in small vesicles inside the cytoplasm. Similar to what had been observed using confocal microscopy (Figure 4), no significant accumulation was found of PLyAd-DOX in the nucleus, and thus no DOX signal was detected from the nucleus after 24 hours of incubation (Figure 5, *G*). Cytoplasmic PLyAd-DOX exhibited a single lifetime distribution peaking at around 3.3 nanoseconds (Figure 5, *H*, *I*).

As control measurements, fluorescence lifetimes were measured in vitro in solutions containing free DOX and double-stranded DNA. Measurements were performed at a range of DNA/DOX ratios. For a fixed amount of DOX solution, the concentration of double-stranded DNA added to the solution was gradually increased. The results are

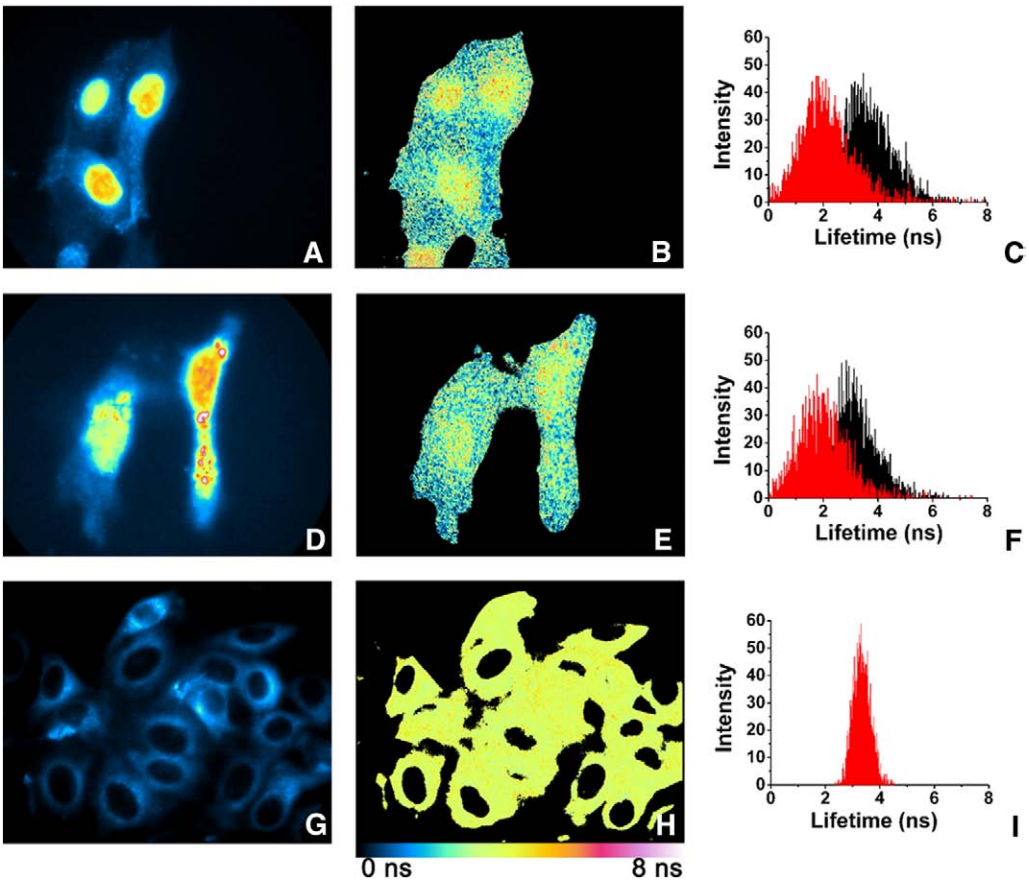

Figure 5. The images of fluorescence intensity (**A, D, G**) and phase lifetime (**B, E, H**) in the Hela cells. The cells were incubated with 0.01 mg mL^{-1} (**A**–**C**), 0.05 mg mL^{-1} (**D**–**F**), free DOX, and 1.0 mg mL^{-1} PLyAd-DOX (**G**–**I**) for 24 hours before lifetime imaging. Corresponding lifetime histograms in nucleus (black) and cytoplasm (red) are summarized in graphs in **C**, **F**, and **I**.

shown in Figure 6, and clearly an increase of the DOX lifetime is seen as the DNA/DOX ratio is increased, increasing from 1.1 nanoseconds to 2.4 nanoseconds at the highest DNA/DOX ratio.

Discussion

DOX is an anthracycline antibiotic that is commonly used in the treatment of a wide spectrum of cancers. The exact mechanism of its antitumor activity still remains unclear. It is known, however, that DOX intercalates into DNA, which results in the blocking of topoisomerase II activity, preventing DNA replication and cell division.[22-24] For encapsulated DOX, its cytotoxicity relies on the amount of drug released in active form inside cells, because the presence of polymer carriers hinders the intercalation of DOX into DNA.

Confocal microscopy revealed differences between the uptake mechanisms of PLyAd-DOX and free DOX. The nuclear accumulation of free DOX can be ascribed to diffusion. In contrast, PLyAd-DOX is taken up by the cells into small vesicles, and concentrations remain mostly in the cytoplasm with negligible nuclear accumulation observed for incubation periods up to 72 hours. These findings are characteristic for uptake of PLyAd-DOX via endocytosis and not via diffusion. The marked difference in fluorescence

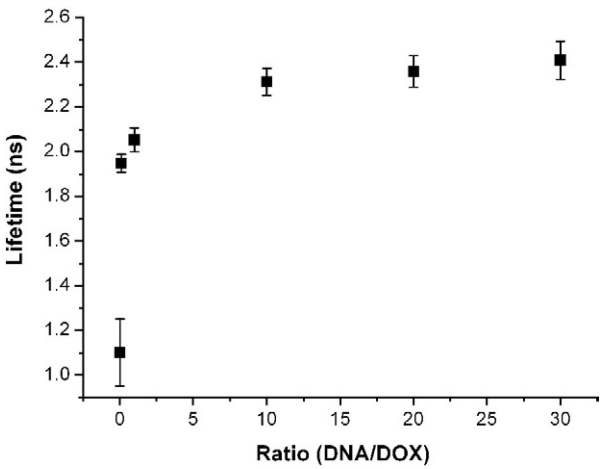

Figure 6. Fluorescence lifetime of DOX when mixed with double-stranded DNA at a range of DNA/DOX ratios.

patterns observed between free DOX and PLyAd-DOX revealed that no significant release of DOX from the internalized PLyAd-DOX took place, and this accounts also for the reduced cytotoxicity during the period of observation. It is interesting to note that the fluorescence intensity of internalized PLyAd-DOX reaches a maximum at around 24 hours, with a continuous decrease then observed on increased incubation periods up to 72 hours. The reason for this is unclear and requires further elucidation.

FLIM was performed of free DOX and PLyAd-DOX at different concentrations in live cells. The bimodal lifetime distribution observed for internalized free DOX (Figure 5, *A–F*) suggests the existence of two different states of DOX within the cells. The lifetime of DOX increased to 1.8 nanoseconds in the cytoplasm and to 3.8 nanoseconds in the nucleus from its corresponding value in aqueous solution (1.1 nanoseconds). The increased lifetime of nuclear DOX compared with cytoplasmic DOX can be ascribed to the known nuclear intercalation effect of DOX with DNA.[25,26] DOX forms π-π stacks with the aromatic groups of the DNA base pairs, locally reducing the exposure of DOX to external quenchers (i.e., dissolved oxygen), and this leads to the observed increases in fluorescence lifetime. Membrane-bound DOX could also be making a contribution to the lifetime increase, in that DOX is positively charged and tends to bind to membranes just like any other positively charged molecule. However, DOX bound to membranes should be localized at the cell periphery and on vesicle membranes. The lifetime increases were globally observed (i.e., from cytoplasmic DOX), and we therefore do not think that membrane-bound DOX is the dominant factor accounting for the observed lifetime increases. Lifetime imaging thus has the power to inform directly on the molecular interactions taking place in complex live-cell systems, and this underlines its potential for use in drug delivery assays.

Increasing the concentration of free DOX leads to decreased lifetimes (Figure 5, *C*, *F*) in the nuclear domains, suggesting the onset of fluorescence self-quenching. Increasing the concentration from 0.01 to 0.05 mg mL^{-1} reduced lifetimes from 3.8 nanoseconds to 2.8 nanoseconds, whereas cytoplasmic lifetimes remained unchanged. Again this demonstrates the potential of lifetime imaging to inform on detailed molecular-level events.

It is seen from Figure 3 that PLyAd-DOX is spectrally indistinguishable from free DOX; however, this is not the case with lifetime imaging. Whereas intensity-based imaging does not allow us to distinguish between the two classes of molecules, their lifetime signatures are substantially different, leading to a clear differentiation between the two species. A PLyAd-DOX concentration of 1.0 mg mL^{-1} yields the same amount of DOX as the free DOX at 0.05 mg mL^{-1}, however the PLyAd-DOX lifetime distribution in the cytoplasm displays a much narrower histogram than corresponding free-DOX concentration after incubation for 24 hours. This narrower distribution peak may be associated with the protected environment that micellar structures give to the loaded fluorophore (DOX), reducing its sensitivity to environmental quenching. The lifetime changes observed of free DOX in the nuclear domain compared with cytoplasmic DOX provide evidence of intercalation of DOX into the DNA strands.

These mechanisms were elucidated further by in vitro lifetime measurements conducted in solutions containing free DOX and DNA at different ratios. Whereas free DOX showed a concentration-independent lifetime of 1.1 nanoseconds in aqueous solution, increases in DOX lifetime were observed on mixing with DNA. This increase is clearly a result of DNA intercalation,[25,26] resulting in an effective shielding of DOX from external quenchers such as oxygen.

The in vitro observations provide foundation for our in vivo observations, explaining both the increasing lifetimes with intercalation and decreasing lifetimes on high drug loading in the nucleus due to increasing self-quenching.

In conclusion, we demonstrate here the use of frequency-domain FLIM for the study of drug delivery systems in living cells. FLIM provides additional information compared with standard intensity-based techniques, informing on the processes occurring on a molecular level. To demonstrate this, we have studied the uptake behavior of micelle-encapsulated PLyAd-DOX and free DOX in living cells. PLyAd-DOX was taken up by cells via endocytosis, and a maximum concentration of the drug was observed after 24 hours of incubation, after which the PLyAd-DOX concentration began to diminish. Uptake of free DOX, in contrast, was observed to occur at a much faster scale by diffusive and active transport processes. The observed lifetime distribution of free DOX in the nuclear domain could be explained by a balance of concentration-dependent self-quenching effects and intercalation of free DOX into DNA, leading to an effective protection against external quenchers. FLIM thus has powerful capabilities in drug delivery research, providing information complementary to purely intensity-based imaging approaches, permitting detailed molecular-level function and interactions to be observed in vivo.

Acknowledgment

The authors gratefully acknowledge Cosimo D'Andrea of the Politecnico di Milano, Italy, for help with the TCSPC measurements.

References

1. Vasey PA, Kaye SB, Morrison R, Twelves C, Wilson P, Duncan R, et al. Phase I clinical and pharmacokinetic study of PK1 [N-(2-hydroxypropyl)methacrylamide copolymer doxorubicin]: first member of a new class of chemotherapeutic agents—drug-polymer conjugates. Clin Cancer Res 1999;5:83-94.
2. Lukyanov AN, Gao Z, Mazzola L, Torchilin VP. Polyethylene glycol-diacyllipid micelles demonstrate increased accumulation in subcutaneous tumors in mice. Pharm Res 2002;19:1424-9.

3. Kakizawa Y, Kataoka K. Block copolymer micelles for delivery of gene and related compounds. Adv Drug Deliv Rev 2002;54: 20-222.
4. Tomlinson R, Heller J, Brocchini S, Duncan R. Polyacetal-doxorubicin conjugates designed for pH-dependent degradation. Bioconjug Chem 2003;14:1096-106.
5. Lukyanov AN, Gao Z, Torchilin VP. Micelles from polyethylene glycol/ phosphatidylethanolamine conjugates for tumor drug delivery. J Control Release 2003;91:97-102.
6. Kaneda Y, Tsutsumi Y, Yoshioka Y, Kamada H, Yamamoto Y, Kodaira H. The use of PVP as a polymeric carric to improve the plasma half-life of drugs. Biomaterials 2004;25:3259-66.
7. Ahmed F, Discher DE. Self-porating polymersomes of PEG-PLA and PEG-PCL: hydrolysis-triggered controlled release vesicles. J Control Release 2004;96:37-53.
8. Veronese FM, Schiavon O, Pasut G, Mendichi R, Andersson L, Tsirk A, et al. PEG-doxorubicin conjugates: influence of polymer structure on drug release, in vitro cytotoxicity, biodistribution, and antitumor activity. Bioconjug Chem 2005;16:775-84.
9. Bader H, Ringsdorf H, Schmidt B, Water soluble polymers in medicine. Angew Chem. 1984;123-124:457-85.
10. Kabanov AV, Chekhonin VP, Alakhov VY, Batrakova EV, Lebedev AS, Melik-Nubarov NS, et al. The neuroleptic activity of haloperidol increases after its solubilization in surfactant micelles: micelles as microcontainers for drug targeting. FEBS Lett 1989;258:343-5.
11. Yokoyama M, Satoh A, Sakurai Y, Okano T, Matsumura Y, Kakizoe T, et al. Incorporation of water-insoluble anti-cancer drug into polymeric micelles and control of their particle size. J Control Release 1998;55:219-29.
12. Calleja V, Ameer-Beg SM, Vojnovic B, Woscholski R, Downward J, Larijani B. Monitoring conformational changes of proteins in cells by fluorescence lifetime imaging microscopy. J Biochem 2003;372:33-40.
13. Vermeer JEM, Van Munster EB, Vischer NO, Gadella Jr TWJ. Probing plasma membrane microdomains in cowpea protoplasts using lipidated GFP-fusion proteins and multimode FRET microscopy. J Microsc 2003; 214:190-200.
14. Lin HJ, Herman P, Lakowicz JR. Fluorescence lifetime-resolved pH imaging of living cells. Cytometry 2003;52A:77-89.
15. Clayton AHA, Hanley QS, Arndt-Jovin DJ, Subramaniam V, Jovin TM. Dynamic fluorescence anisotropy imaging microscopy in the frequency domain (rFLIM). J Biophys 2002;83:1631-49.
16. Campbell A, Uttamchandani D. Optical dissolved oxygen lifetime sensor based on sol-gel immobilization. Science, Measurement and Technology, IEE Proc 2004;151:291-7.
17. Hanley QS, Subramaniam V, Arndt-Jovin DJ, Jovin TM. Fluorescence lifetime imaging: multi-point calibration, minimum resolvable differences, and artifact suppression. Cytometry 2001;43:248-60.
18. Eccleston ME, Kuiper M, Gilchrist FM, Slater NKH. pH-responsive pseudo-peptides for cell membrane disruption. J Control Release 2000; 69:297-307.
19. Swartling J, Bassi A, D'Andrea C, Pifferi A, Torricelli A, Cubeddu R. Dynamic time-resolved diffuse spectroscopy based on supercontinuum light pulses. Appl Opt 2005;44:4684-92.
20. Elder AD, Matthews SM, Swartling J, Yunus K, Frank JH, Brennan CM, et al. Application of fluorescence lifetime imaging microscopy as a quantitative analytical tool for microfluidic devices. Opt Express 2006; 14:5456-67.
21. Elder AD, Frank JH, Swartling J, Dai X, Kaminski CF. Calibration of a wide-field frequency-domain fluorescence lifetime microscopy system using light emitting diodes as light sources. J Microsc 2006;224:166-80.
22. Claires JB, Dattagupta N, Crothers DM. Studies on interaction of anthracycline antibiotics and deoxyribonucleic acid: equilibrium binding studies on the interaction of daunomycin with deoxyribonucleic acid. Biochemistry 1982;21:3933-40.
23. Ross WE. DNA topoisomerases as targets for cancer therapy. Biochem Pharmacol 1985;34:4191-5.
24. Bodley A, Liu LF, Israel M, Seshadri R, Koseki Y, Giuliani FC, et al. DNA topoisomerase II-mediated interaction of doxorubicin and daunorubicin congeners with DNA. Cancer Res 1989;49:5969-78.
25. Ashikawa I, Kinosita K, Ikegami A. Increased stability of the higher order structure of chicken erythrocyte chromatin: nanosecond anisotropy studies of intercalated ethidium. Biochemistry 1985;24:1291-7.
26. Malatesta V, Andreoni A. Dynamics of anthracyclines/DNA interaction: a laser time-resolved fluorescence study. Photochem Photobiol 1988;48: 409-15.